REPORT DOCUMENTATION PAGE		READ INSTRUCTIONS BEFORE COMPLETING FORM
1. REPORT NUMBER NRL Memorandum Report 5155	2. GOVT ACCESSION NO.	3. RECIPIENT'S CATALOG NUMBER
4. TITLE (and Subtitle) PLASMA EFFECTS ON LEVEL SHIFTS OF H AND He$^+$		5. TYPE OF REPORT & PERIOD COVERED Interim report on a continuing NRL problem.
		6. PERFORMING ORG. REPORT NUMBER
7. AUTHOR(s) M. Blaha* and J. Davis		8. CONTRACT OR GRANT NUMBER(s)
9. PERFORMING ORGANIZATION NAME AND ADDRESS Naval Research Laboratory Washington, DC 20375		10. PROGRAM ELEMENT, PROJECT, TASK AREA & WORK UNIT NUMBERS 61153N; RR011-09-41; 47-0911-0-3
11. CONTROLLING OFFICE NAME AND ADDRESS Office of Naval Research Arlington, VA 22217		12. REPORT DATE August 24, 1983
		13. NUMBER OF PAGES 31
14. MONITORING AGENCY NAME & ADDRESS(if different from Controlling Office)		15. SECURITY CLASS. (of this report) UNCLASSIFIED
		15a. DECLASSIFICATION/DOWNGRADING SCHEDULE

16. DISTRIBUTION STATEMENT (of this Report)

Approved for public release; distribution unlimited.

17. DISTRIBUTION STATEMENT (of the abstract entered in Block 20, if different from Report)

19. KEY WORDS (Continue on reverse side if necessary and identify by block number)

Level shifts   Plasma
H   Polarization
He$^+$

20. ABSTRACT (Continue on reverse side if necessary and identify by block number)

  Level shifts of hydrogen and ionized helium due to plasma interaction have been calculated for the electron density 10^{17} cm^{-3} using the spherically symmetrical distribution of charged particles around the radiating atom. The plasma electron density has been obtained from the solution of the Schrödinger equation and the ion density from the Boltzmann distribution function. In both cases, the effective

(Continues)

DD _{1 JAN 73} FORM 1473 EDITION OF 1 NOV 65 IS OBSOLETE
S/N 0102-014-6601

20. ABSTRACT (Continued)

potential for plasma particles has been determined from the nuclear charge
of the radiator and from the screening by the bound electron. Relative
level shifts (i.e., shifts with respect to the ground level) are presented as
a function of temperature. The effect of replacing the screened potential
by the true interatomic potential on the ion distribution and level shifts
is discussed.

CONTENTS

Accesion For		
NTIS CRA&I	☒	
DTIC TAB	☐	
Unannounced	☐	
Justification		
By		
Distribution /		
Availability Codes		
Dist	Avail and / or Special	
A-1		

PLASMA EFFECTS ON LEVEL SHIFTS OF H AND He$^+$

I. Introduction

The interaction of plasma microfields with highly charged ions is attracting considerable attention in dense plasma physics research, particularly in the diagnostic area of laser driven pellet implosions where it is anticipated that electron densities will exceed 10^{24} cm^{-3}. It is fairly well established that as the electron density increases to values in excess of say above 10^{16} cm^{-3}, a host of effects onset that cause atomic energy level splitting, shifting and broadening, spectral line profile modifications, level merging, and ionization lowering as well as a variety of other many-body phenomena. All these effects are, of course, related and probably derive from a single unified theory. However, in the absence of such a theory, each process is generally treated individually and compared with experimental results and other theoretical calculations in the hope of gaining further insight into the dense plasma physics influence on fundamental atomic structure and processes. In addition to the basic and fundamental nature of this problem, there is an immediate and applied aspect also. The spectroscopy of dense hot plasmas still remains one of the most viable, and oftentimes the only, means of diagnosing conditions within the plasmas' interior. Therefore, it is essential that we explore the possibilities of extending conventional theoretical spectroscopic techniques into regions of higher density.

In this paper we will focus attention on level shifts. While the broadening of spectral lines is thought to be better understood concept-ually, the line shift still remains a rather controversial subject both theoretically as well as experimentally. We will assume that in dense plasmas, atomic level shifts are the results of the following effects: (a) Quadratic Stark effect, (b) ion quadrupole interaction, (c) electron colli-sions, and (d) plasma polarization in the vicinity of the radiating atom. Oftentimes processes (a)-(d) collectively are referred to as the "plasma polarization shift" (PPS). In very dense plasmas ($N_e \gtrsim 10^{24}$ cm^{-3}), the individual effects cannot, strictly speaking, be separated from each other, as is done at moderate and low densities ($N_e < 10^{18}$ cm^{-3}), and studied

separately. We will be more restrictive and assume the PPS to refer only to process (d), i.e., the contribution to level shifts arising from nonuniform charge distribution in the neighborhood of the radiator.

The status of the PPS prior to 1980 has been reviewed by Griem[1] and Volonté[2]. A number of estimates of level shifts due to plasma polarization are based on the hydrogenic effective charge approximation in which the effects of electric charges outside the bound electron orbit are ignored. The PPS is then derived under various assumptions according to the form of the free electron charge distribution inside the orbit. More recently, there is a paper by Cauble[3] that includes the electric charge both inside and outside the bound electron orbit. Although this calculation is not self-consistent in the sense that it is a static model and does not account for charge redistribution, it does suggest that the contribution to the level shift is dominated by the charges outside the orbit causing a red rather than blue shift of the Lyman lines of ionized helium. Also, it is worth noting that, except under special conditions, the effect of external charges may be quite different when the atom is in either the upper and lower level, respectively, and may contribute to the observed line shift. A completely different model of the PPS based on the concept of the quantum energy pressure has been introduced by Henry[4], but even this model does not represent a fully quantum-mechanical solution of the problem. However, despite a number of simplifying assumptions in existing calculations, some of the theoretical estimates of the PPS have met with a certain degree of success in the case of ionized helium lines.[4-7]

In this investigation we will focus on the sensitivity of the PPS to various forms of the electron and ion distributions, particularly on low lying levels (n = 1 to 4) of hydrogen and ionized helium. In our approach, the energy matrix element is evaluated for the interaction of the single bound electron with the time averaged potential due to the plasma electrons and ions. For simplicity, it is assumed that the distribution of electric charges around the radiating atom is spherically symmetric. Similar assumptions were invoked by Griem[1], Berg et al.[8], Greig et al.[9], Burgess and Peacock[10], Volonté[7], and Pittman et al.[11] Both space and time averaging of the potential is a questionable procedure for several reasons. While the deBroglie wavelength of thermal electrons may be

comparable to the dimensions of the radiator, providing some justification for the continuous nature of the distribution of electric charge, the discrete nature of the ion charges is completely ignored in our calculation. At small distances, the radiator and perturbing ion may instantaneously form a quasimolecular system giving rise to close satellite lines instead of a shift of the whole line. Also, if the duration of the interaction is short compared to the period of the orbital motion, then the time averaging of the perturbing potential is clearly an inadequate procedure. In spite of these obstacles, it should be possible within the present calculational framework to obtain reasonable estimates of the PPS. It may also provide guidance to more detailed and mature investigations in the future.

In low density plasmas ($N_e < 10^{18}$ cm^{-3}) the Debye shielding distance is much larger than the dimensions of the radiating atom and the level shifts are produced mainly by the charge distribution in the vicinity of the radiator. The method utilized here treats the motion of the plasma electrons quantum mechanically while the ions are described by classical Boltzmann statistics. Also, the potential for both the free electrons and ions is derived from the nuclear charge and from the screening by the bound electron. The effects of the ion distribution based on interatomic potentials are included in several examples. Finally, the mutual interaction of plasma electrons as well as that of the ions is neglected and consequently near the radiator no account is taken of collisional redistribution of electron velocities.

II. General Considerations

In this calculation of atomic level shifts in one-electron systems due to the plasma polarization effect we adopt the simplifying assumption that the actual distribution of perturbing charges around the radiating atom can be replaced by a continuous, spherically symmetric time independent charge distribution. Even with this assumption, the problem of calculating atomic level shifts may be approached from two different viewpoints: either the charge distribution around the radiator corresponds to an average state of excitation of the radiating atom (case A), or it corresponds to a partic-ular level $n\ell$ of the radiator (case B). Case A is equivalent to the assumption that plasma particles do not have time to adjust to individual atomic orbitals.

3

We will assume that only singly charged ions are present in the plasma which may be partially ionized, and that the effect of neutral atoms surrounding the radiator may be neglected.

The total energy $E_{n\ell}$ of the system consisting of the $n\ell$-bound electron in the field of the nuclear charge Z and the surrounding plasma in a given volume may be written as a sum

$$E_{n\ell} = E_1 + E_2 + E_3 + E_4 , \tag{1}$$

where E_1 is the expectation value of the operator $-\frac{1}{2} \nabla^2 - Z r^{-1}$ (in atomic units, which are used throughout the paper, unless indicated otherwise) evaluated with the wave function of the bound electron in the $n\ell$ orbit, E_2 represents the electrostatic interaction between the bound electron and the plasma, E_3 is the interaction energy of the nucleus and the plasma, and E_4 is the sum of all contributions not explicitly included in E_1, E_2, or E_3. Effects of exchange between the bound and free electrons will be omitted in the present calculations. In the first approximation, the energy of an emitted or absorbed photon is equal to

$$
\begin{aligned}
E_{n\ell} - E_{n'\ell'} = {} & (E_1 + E_2 + E_3 + E_4)_{n\ell} \\
& - (E_1 + E_2 + E_3 + E_4)_{n'\ell'}
\end{aligned}
\tag{2}
$$

where the quantities in parentheses $(\ )_{n\ell}$ and $(\ )_{n'\ell'}$ are to be evaluated with respect to the $n\ell$ and $n'\ell'$ atomic level, respectively. In most experimental plasma conditions in which neutral hydrogen and singly ionized helium are observed, the perturbation of atomic wave functions is very small and we can assume that $(E_1)_{n\ell}$ is equal to the eigenvalue $\varepsilon_{n\ell}$ of the unperturbed Schrödinger equation for the hydrogen-like atom.

The frequency shift $\Delta\nu$ of a spectral line due to the plasma interaction is then equal to

$$\Delta\nu = h^{-1}(E_{n\ell} - E_{n'\ell'} - \varepsilon_{n\ell} + \varepsilon_{n'\ell'}) .$$

4

Because only energy differences are directly observable, it is convenient to express all energies $E_{n\ell}$ with respect to the energy of the ground level 1s. As a relative shift of the $n\ell$ level we define a quantity

$$\Delta E'_{n\ell} = E_{n\ell} - E_{1s} - (\varepsilon_{n\ell} - \varepsilon_{1s}) , \qquad (3)$$

so that

$$\Delta\nu = h^{-1} \Delta E'_{n\ell} ,$$

if $n\ell \to 1s$ is an optical transition.

III. $\underline{\text{Method of Calculation}}$

Define

$$W(r) = Zr^{-1} + 4\pi r^{-1} \int_0^r \rho(r') r'^2 dr' + 4\pi \int_r^\infty \rho(r') r' dr' . \qquad (4)$$

$\rho(r') = \rho_e(r') + \rho_i(r')$, where ρ_e and ρ_i are the spherically averaged charge densities of the plasma electrons and ions, respectively. The potential energy V_b of the bound electron in the field of plasma particles is given by

$$V_b = -W + Zr^{-1} . \qquad (5)$$

We assume that the plasma electrons have a Maxwellian velocity distribution at large distances from the nucleus and that in the vicinity of the radiating atom, in a low-density plasma, ρ_e and ρ_i are determined only by the electrostatic potential of the nucleus and the bound electron. The mutual interaction of plasma electrons and ions will be ignored. Consequently, the potential used for the calculation of ρ_e and ρ_i behaves like $(Z-1)/r$ at large r, while in a real plasma this interaction leads to the formation of a charged cloud and to a faster decrease of potential. In low-density helium plasmas with Z=2 the dimensions of this cloud are several orders of magnitude larger than the size of low lying

5

atomic orbitals and the effect of distant charges on relative atomic energy levels will be ignored.

In our procedure, ρ_e is defined by

$$\rho_e(r) = -N_e \int_0^\infty f(k) \, (kr^2)^{-1} \sum_{\ell=0}^\infty (2\ell+1) \, F_{k\ell}^2(r) \, dk, \qquad (6)$$

where $f(k)$ is the velocity distribution of free electrons normalized to unity, N_e is the average number density of plasma electrons, and the functions $F_{k\ell}$ are solutions of the equation

$$[\frac{d^2}{dr^2} - \frac{\ell(\ell+1)}{r^2} - 2V_e + k^2] \, F_{k\ell}(r) = 0 \qquad (7)$$

with the asymptotic form

$$F_{k\ell}(r) \sim k^{-1/2} \sin(kr + \delta_{k\ell}) . \qquad (8)$$

For scattering on a neutral target, $\delta_{k\ell}$ is independent of r. From (6), (7) and (8) it follows that $\rho_e \to -N_e$ at large values of r. V_e in Eq. (7) is the potential energy of the plasma electron in the field of the nucleus and the bound electron. If ρ_b is the spherically averaged charge density of the bound electron, V_e is given by

$$V_e(r) = -W(r) \qquad (9)$$

with ρ in expression (4) for $W(r)$ replaced by ρ_b.

CASE A.

In this case, E_3 and E_4 are independent of $n\ell$ and $\Delta E_{n\ell}^-$ is given by

$$\Delta E_{n\ell}^- = (E_2)_{n\ell} - (E_2)_{1s} = \int (P_{n\ell}^2 - P_{1s}^2) \, V_b \, dr . \qquad (10)$$

$P_{n\ell}(r)$ and $P_{1s}(r)$ are unperturbed radial functions of the bound electron normalized to satisfy the condition $\int P_{n\ell}^2 \, dr = 1$, and $V_b(r)$, given by Eq. (5), is the potential energy of the bound electron at a distance r from the nucleus in the field created by plasma electrons and ions.

ρ_b may be written as

$$\rho_b = - (4\pi r^2)^{-1} \sum_{n\ell} b_{n\ell} P^2_{n\ell} (r), \tag{11}$$

where the occupation numbers satisfy the condition $\sum_{n\ell} b_{n\ell} = 1$. In a low-density, low-temperature plasma, the occupation of excited states is very small and we will assume that only the ground level 1s is occupied.

With the assumption that only singly ionized ions are present in the plasma, we adopt the following form for the positive ion charge distribution:

$$\rho_i = N_e \exp (-V_i/kT), \tag{12}$$

where $V_i(r)$ is the interatomic potential for the radiating atom and a plasma ion. In our procedure

$$V_i(r) = -V_e(r). \tag{13}$$

CASE B.

All three quantities E_2, E_3 and E_4 may depend on $n\ell$ as well as the potential energy $V_b(r)$. We restrict our investigation to the calculation of the quantity $(E_2)_{n\ell} - (E_2)_{1s}$ as in case A, and adopt the assumption that the sum E_3+E_4 does not depend on $n\ell$. Then

$$\Delta E'_{n\ell} = \int [(V_b)_{n\ell} P^2_{n\ell} - (V_b)_{1s} P^2_{1s}] \, dr \tag{14}$$

with V_b defined by (5). Furthermore,

$$\rho_b = - (4\pi r^2)^{-1} P^2_{n\ell} (r) , \tag{15}$$

and ρ_i, V_i are defined by (12) and (13). In case B, both V_e and V_i depend on the state of the radiator.

Eq. (13) implies that the bound state wave function $P_{n\ell}$ remains essentially unperturbed by plasma ions. Other forms of interatomic potential V_i will be discussed in the Appendix.

The charge profile in (6) was obtained numerically from 7 different values of k for which Eq. (7) has been solved. Number of angular momenta included in the summation over ℓ in (6) varied from 10 to 50 for hydrogen and from 20 to 60 for ionized helium, depending on k.

IV. Results for Hydrogen and Ionized Helium.

Calculations of relative level shifts have been made for hydrogen for temperatures from 0.5 to 2.0 eV and for singly ionized helium from 2.5 to 4.0 eV. Since the relative shifts in low-density plasmas are proportional to the average electron density N_e (see Eqs. (4), (5), (10), (12)), our results are normalized to $N_e = 10^{17}$ cm^{-3}. Relative level shifts $\Delta E'_{n\ell}$ for case A are shown in Figs. 1 and 3 for H and He$^+$, respectively, and for case B are displayed on Figs. 2 and 4.

Plasma interactions remove the degeneracy of ℓ-sublevels. In our approximation all effects of level broadening are ignored and the splitting is well defined.

In case A, relative level shifts for both hydrogen and ionized helium are negative and lead to the red shift of spectral lines of the Lyman series. The ℓ-splitting of relative level shifts due to plasma interactions is generally larger for He$^+$ than for H, and the values of $\Delta E'_{n\ell}$ increase with ℓ.

In case B, the behavior of relative shifts for hydrogen is drastically changed. Almost all values of $\Delta E'_{n\ell}$ are positive, the ℓ-splitting is so large that some curves corresponding to different principal quantum numbers cross each other, and relative shifts $\Delta E'_{n\ell}$ increase with decreasing ℓ. For ionized helium, case B is not much different from case A due to the dominant attractive force of the nuclear charge. All $\Delta E'_{n\ell}$ values are slightly shifted upwards but remain negative as in case A.

When comparing the present results with the observed line shifts, one has to bear in mind that (a) using differences of level shifts to calculate line shifts represents only an approximation, (b) other effects mentioned

8

in the introduction contribute to the line shifts and may be larger or comparable to the values of $\Delta E'_{n\ell}$, and (c) our relative shifts $\Delta E'_{n\ell}$ in case B (Figs. 2 and 4) do not include contributions from E_3 and E_4 in Eq. (2).

For He$^+$, our results predict a very small red shift of Lyman series lines. The shifts are of the same order of magnitude as those obtained from the Debye-Hückel potential. The experimental evidence, however, points to much larger blue shifts[2,5]. For the 3 - 2 transition of He$^+$ at 1640 Å our calculations predict a negligible red shift in agreement with experiment[6], but the theoretical shift for the 4 - 2 transition at 1215 Å is again too small, except possibly for the temperature around 4 eV. Pittman et al.[11,12] measured a red shift of 0.17 Å for the transition 4 - 3 at 4686 Å for T = 4 eV in He$^+$. However, the ion contribution itself (quadrupole and quadratic) has been estimated [12] to be -0.24 Å, so that our theoretical result +0.11Å for the 4f-3d component (Fig. 3) for the PPS cannot explain the observed red shift. Wiese et al.[16] also measured red shift of Balmer series lines of hydrogen. Our theoretical results predict blue shifts for H$_\alpha$ and either blue or red shifts for Hβ, depending on temperature and line component, but the calculated values are much smaller than the observed ones. Measurements of the L$_\alpha$ shifts of hydrogen have been reported by Fussman[13]. The blue shift, if any, was found to be less than 0.015Å at T = 1eV which agrees with our theoretical estimates.

We arrive at the conclusion that the PPS for hydrogen and ionized helium as defined in the present investigation is too small to be responsible for the majority of measured line shifts in contrast to the results of theories based on the hydrogenic effective charge approximation, and that other mechanisms have to be taken into account in order to obtain an agreement with observations. A similar conclusion has been reached by Cauble[3] who calculated the PPS for He$^+$ by a method similar to that of Volonté[7], but included screening effects of plasma electrons outside the orbit of the bound electron.

In the present investigation, the potential energy V_i for the ion distribution in (12) was derived from the screening by the bound electron, and it was assumed that the bound electron wave function remained unperturbed during collisions with ions. Consequently there was no difference between level shifts obtained for helium ions in a pure helium

plasma, and for helium ions in a hydrogen plasma containing helium ions only as impurities. In the Appendix we will investigate the effects of ions on level shifts by substituting actual interatomic potentials for V_i in Eq. (12).

V. Appendix

During close collisions with ions, the bound electron wave functions may be appreciably distorted by the strong electric field of the colliding ion. In some cases a quasimolecule may be temporarily formed. The short-range effects may influence the distribution of ions around the radiating atom and can be taken into account, in the first approximation, by replacing V_i in Eq. (12) by true interatomic potentials.

Generally, more than one potential curve corresponds to a particular $n\ell$ state of a hydrogen atom or a hydrogenic ion and a plasma ion in its ground state. Each of these potential curves is associated with a different state of the united atom as the nuclear separation approaches zero. E.g., there are two potential curves correspponding to a hydrogen atom in the ground state, and a proton, associated with the $1s\sigma_g$ and $2p\sigma_u$ states of the H_2^+ molecule. Instead of using Eq. (12), in this case we calculate the ion charge distribution from the relation

$$\rho_i = N_e (\textstyle\sum_j g_j)^{-1} \textstyle\sum_j g_j \exp [-V_i(A_j)/kT] , \qquad (16)$$

where $V_i(A_j)$ is the interatomic potential energy corresponding to the molecular state A_j with the statistical weight g_j, and the summation is carried out over all molecular states leading to the same state of separated atoms.

Potential curves $V_i(A_j)$ for helium ions in a pure helium plasma correspond to the process $He_2^{++} \rightarrow He^+(n\ell) + He^+(1s)$. However, sufficient data on interatomic potentials for excited states of He_2^{++} are not available, and therefore we restrict our calculations of He^+ level shifts to the case of impruity helium ions in a hydrogen plasma. In this case we consider potential curves for the process $HeH^{++} \rightarrow He^+(n\ell) + H^+$, and use potentials calculated by Bates and Carson[14] for $n\ell = 1s$, 2s, and 2p.

For relative level shifts in hydrogen, we consider the process $H_2^+ \rightarrow H(n\ell) + H^+$. The interatomic potentials are taken from Bates et al.[15] for $n\ell = 1s$, 2s, 2p, and 3s. The published potential curves were extrapolated to larger values of nuclear separation, where needed.

The interatomic potentials $V_i(A_j)$ are compared with the screened potentials used in par. 4 in Figs. 5 - 10.

The ion distribution calculated from (16) using interatomic potentials has a profound effect on the relative level shifts. As in the text, we consider two cases: in case A, the relative level shifts $\Delta E'_{n\ell}$ for all $n\ell$ levels are calculated from the same $V_b(r)$. The distribution of plasma electrons, given by (6), is obtained from the screening by the 1s bound electron, and the distribution of ions, given by (16), is obtained from the interatomic potentials corresponding to $H(1s) + H^+$ or $He^+(1s) + H^+$, respectively. In case B, the potential energies $V_b(r)$ corresponding to different $n\ell$ levels are different. For a given $n\ell$ level, the distribution of plasma electrons is determined from the screening by the $n\ell$ bound electron, and the ion distribution by interatomic potentials corresponding to $H(n\ell) + H^+$ or $He^+(n\ell) + H^+$. Results for $\Delta E'_{n\ell}$ calculated from (10) or (14), respectively, are shown in Figs. 11-14.

The attractive character of the potential curve for the $1s\sigma_g$ state of H_2^+ at small r (Fig. 5) leads to the accumulation of protons in the vicinity of the hydrogen atom in the ground state and to the lowering of the 1s level. Therefore all relative shifts $\Delta E'_{n\ell}$ rapidly increase with decreasing temperature as shown on Figs. 11 and 12. The large difference of $\Delta E'_{2s}$ and $\Delta E'_{2p}$ in hydrogen (case B, Fig. 12) is the result of the same effect: potential curves of $H(2s)+H^+$ are repulsive, while the curves representing the $2p\pi_u$ and $3d\sigma_g$ states of the $H(2p)+H^+$ system exhibit minima. Consequently the upward shift of the 2p level is reduced by the accumulation of positive charges, and $\Delta E'_{2p} < \Delta E'_{2s}$.

The potential curve corresponding to $He^+(1s)+H^+$ has no minimum and the values of relative shifts for He^+ (Figs. 13,14) do not increase towards lower temperature in contrast to hydrogen. This interatomic potential is very similar to the potential obtained from the simple screening by 1s electron (Fig. 8) and therefore there is not much difference between $\Delta E'_{n\ell}$ on Fig. 3 and 13. The large differences of $\Delta E'_{2s}$ and $\Delta E'_{2p}$ in case B (Fig. 14) again arises from the difference of potential curves associated with the $He^+(2s)+H^+$ and $He^+(2p)+H^+$ systems.

In spite of these changes in relative level shifts, the general conclusion about the magnitude of the shifts obtained within our approximation, which has been discussed earlier, remains valid. The calculated relative shifts of levels for which the interatomic potentials V_i are known, appear to be small and additional mechanisms must be considered for the explanation of measured line shifts.

VI. Acknowledgment

VII. References

1. H.R. Griem, "Spectral Line Broadening by Plasmas" (Academic Press, New York 1974).

2. S. Volonté, J. Phys. D: Appl. Phys. $\underline{11}$,1615 (1978).

3. R. Cauble, J. Quant. Spectrosc. Radiat. Transfer $\underline{28}$,41 (1982).

4. B.I. Henry, Laser and Particle Beams $\underline{1}$,11 (1983).

5. M. Neiger and H.R. Griem, Phys. Rev. A$\underline{14}$,291 (1976).

6. J.R. VanZandt, J.C. Adcock, Jr., and H.R. Griem, Phys. Rev. A$\underline{14}$,2126 (1976).

7. S. Volonté, J. Phys. B: Atom. Molec. Phys. $\underline{8}$,1170 (1975).

8. H.F. Berg, A.W. Ali, R. Lincke, and H.R. Griem, Phys. Rev. $\underline{125}$,199 (1962).

9. J.R. Greig, H.R. Griem, L.A. Jones, and T. Oda, Phys. Rev. Lett. $\underline{24}$,3 (1970).

10. D.D. Burgess and N.J. Peacock, J. Phys. B: Atom. Molec. Phys.$\underline{4}$,L94 (1971).

11. T.L. Pittman, P. Voigt, and D.E. Kelleher, Phys. Rev. Lett. $\underline{45}$,723 (1980).

12. T.L. Pittman, and D.E. Kelleher, NBS preprint (1980).

13. G. Fussman, J. Quant. Spectrosc. Rad. Transfer $\underline{15}$,791 (1975).

14. D.R. Bates and T.R. Carson, Proc. Roy. Soc. Lond. A$\underline{234}$,207 (1956).

15. D.R. Bates, K. Ledsham and A.L. Stewart, Phil. Trans. Roy. Soc. Lond. A$\underline{246}$,215 (1953).

16. W.L. Wiese, D.E. Kelleher, and D.R. Paquette, Phys. Rev. A$\underline{6}$,1132 (1972).
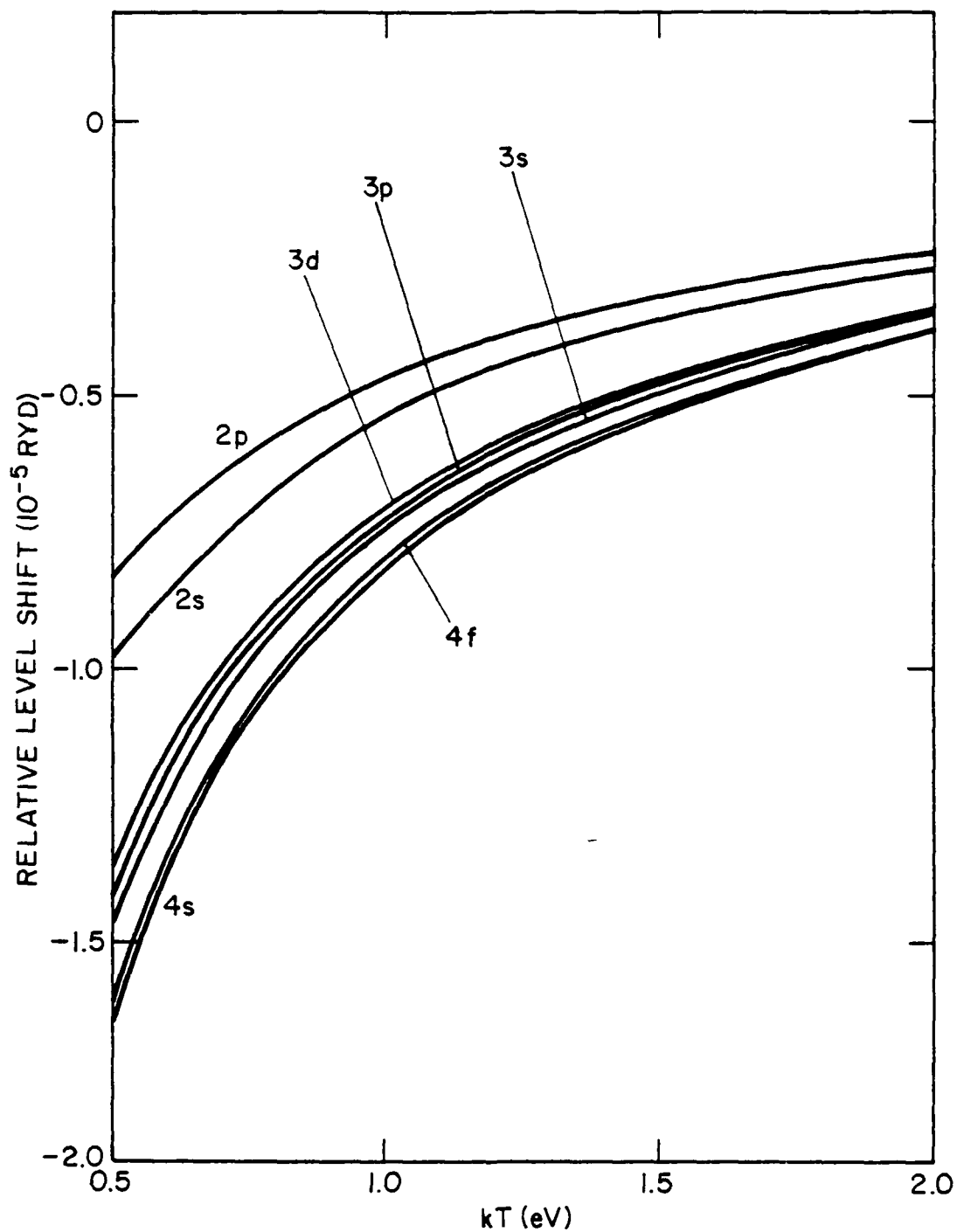
Fig. 1. Relative level shifts $\Delta E'_{n\ell}$ for hydrogen. Hydrogen plasma, $N_e =$ $10^{17} cm^{-3}$. Case A (All relative shifts are calculated from the same perturbing potential. The distribution of plasma electrons and ions around the radiating atom is determined from screening by the 1s bound electron). The curves for 4p and 4d lie between those for 4s and 4f. They are not shown for clarity.

15
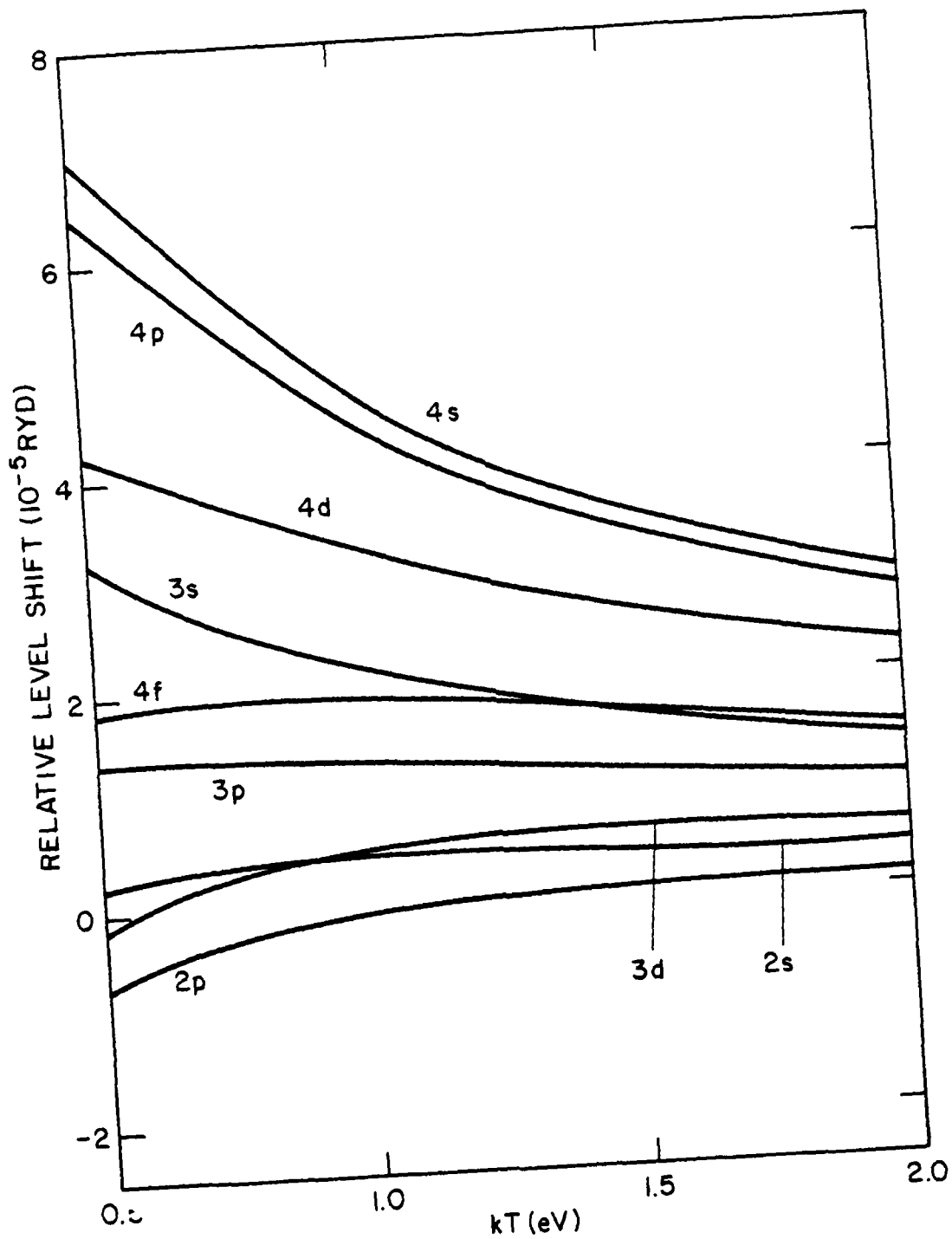
Fig. 2. Relative level shifts $\Delta E^-_{n\ell}$ for hydrogen. Hydrogen plasma, $N_e = 10^{17} cm^{-3}$. Case B (Each quantity $(E_2)_{n\ell}$ in Eq. (14) is calculated from a potential corresponding to the electron and ion distribution derived from screening by the $n\ell$ bound electron).

16
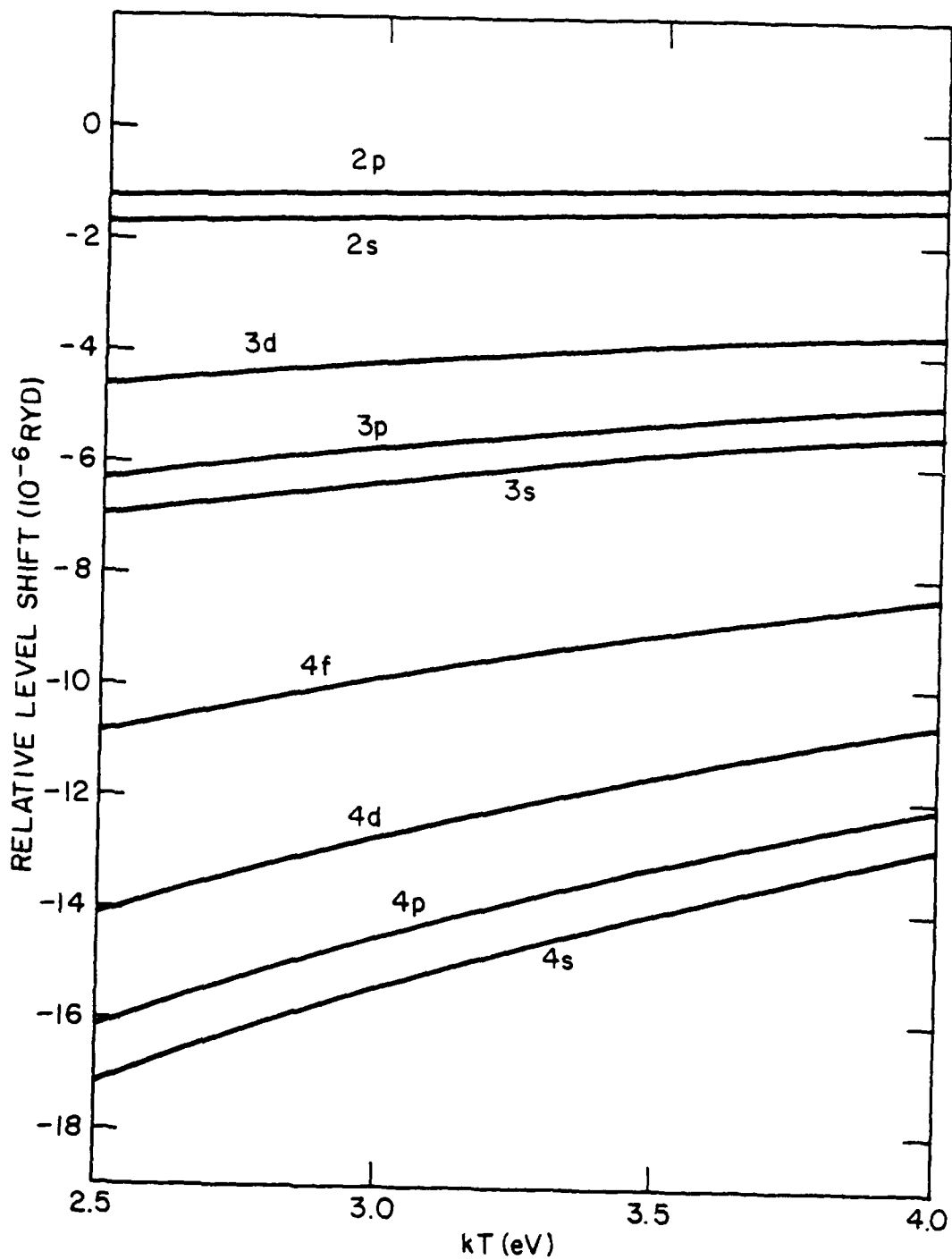
Fig. 3. Relative level shifts $\Delta E_{n\ell}'$ for ionized helium. Hydrogen or helium plasma, $N_e = 10^{17} cm^{-3}$. Case A.
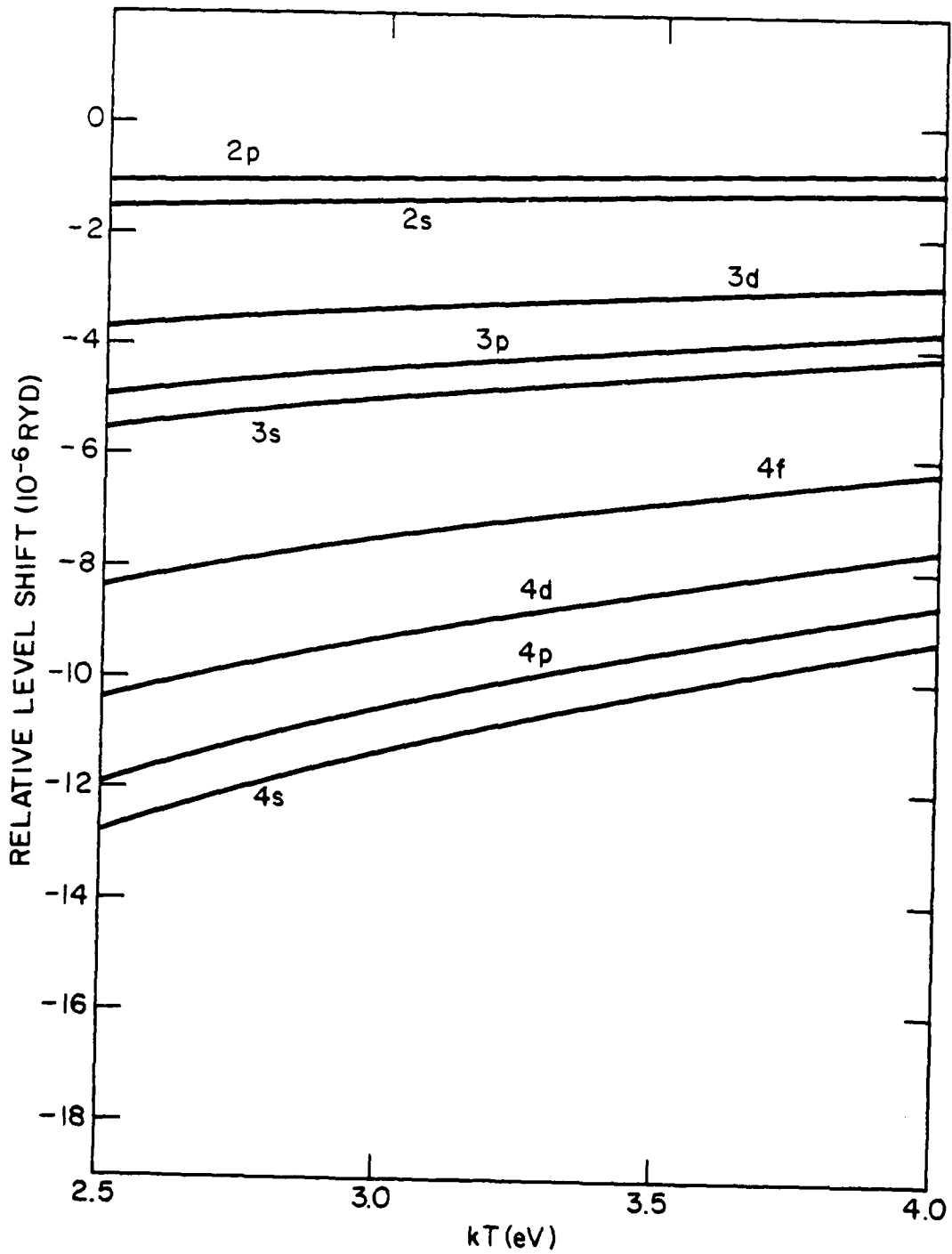
Fig. 4. Relative level shifts $\Delta E_{n\ell}^{-}$ for ionized helium. Hydrogen or helium plasma, $N_e = 10^{17} cm^{-3}$. Case B.
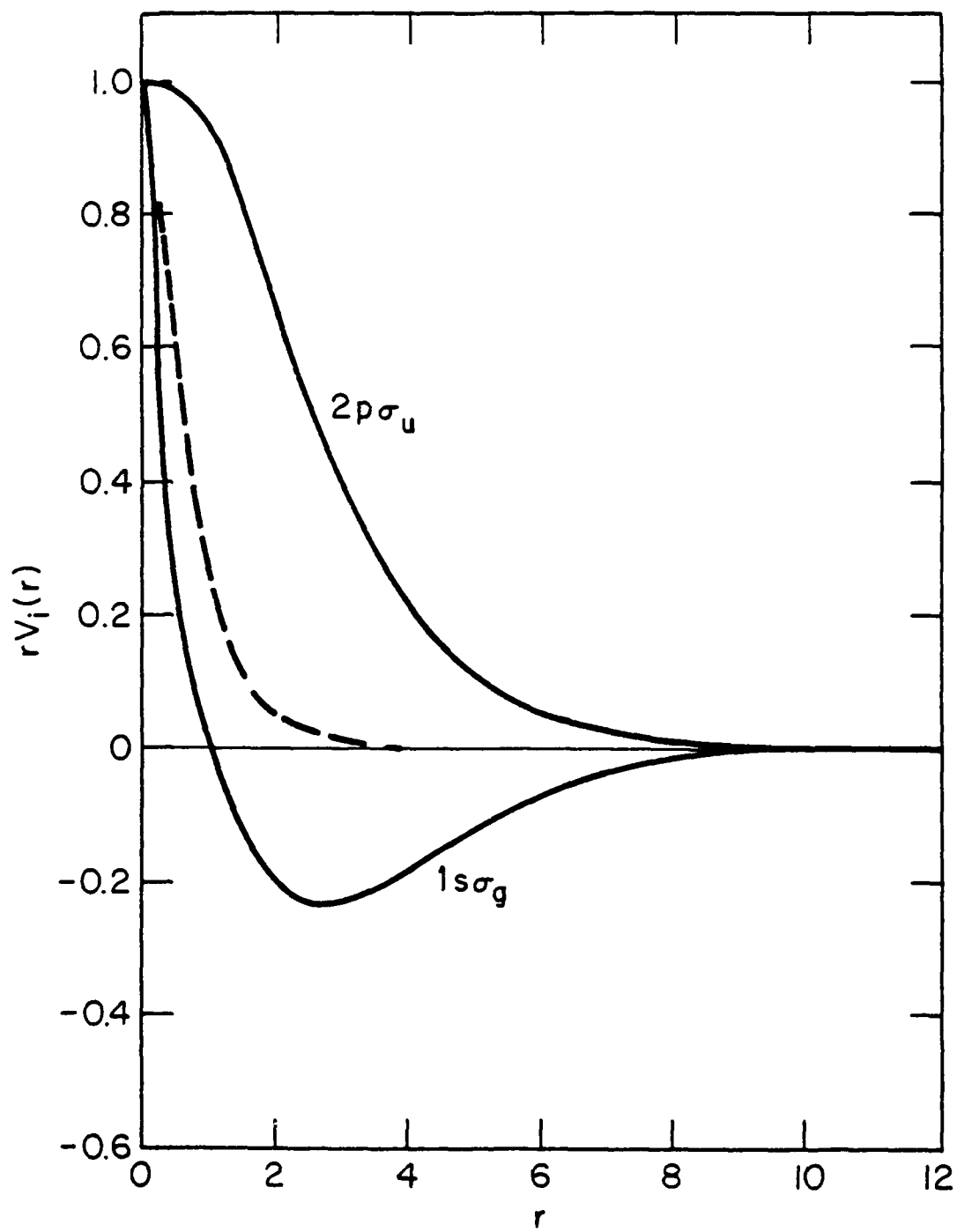
Fig. 5. Effective charge acting on the proton in the system $H(1s) + H^+$. Full curves: Interatomic potentials V_i from Ref. 15. Dashed curve: Potential V_i derived from screening by the 1s bound electron.
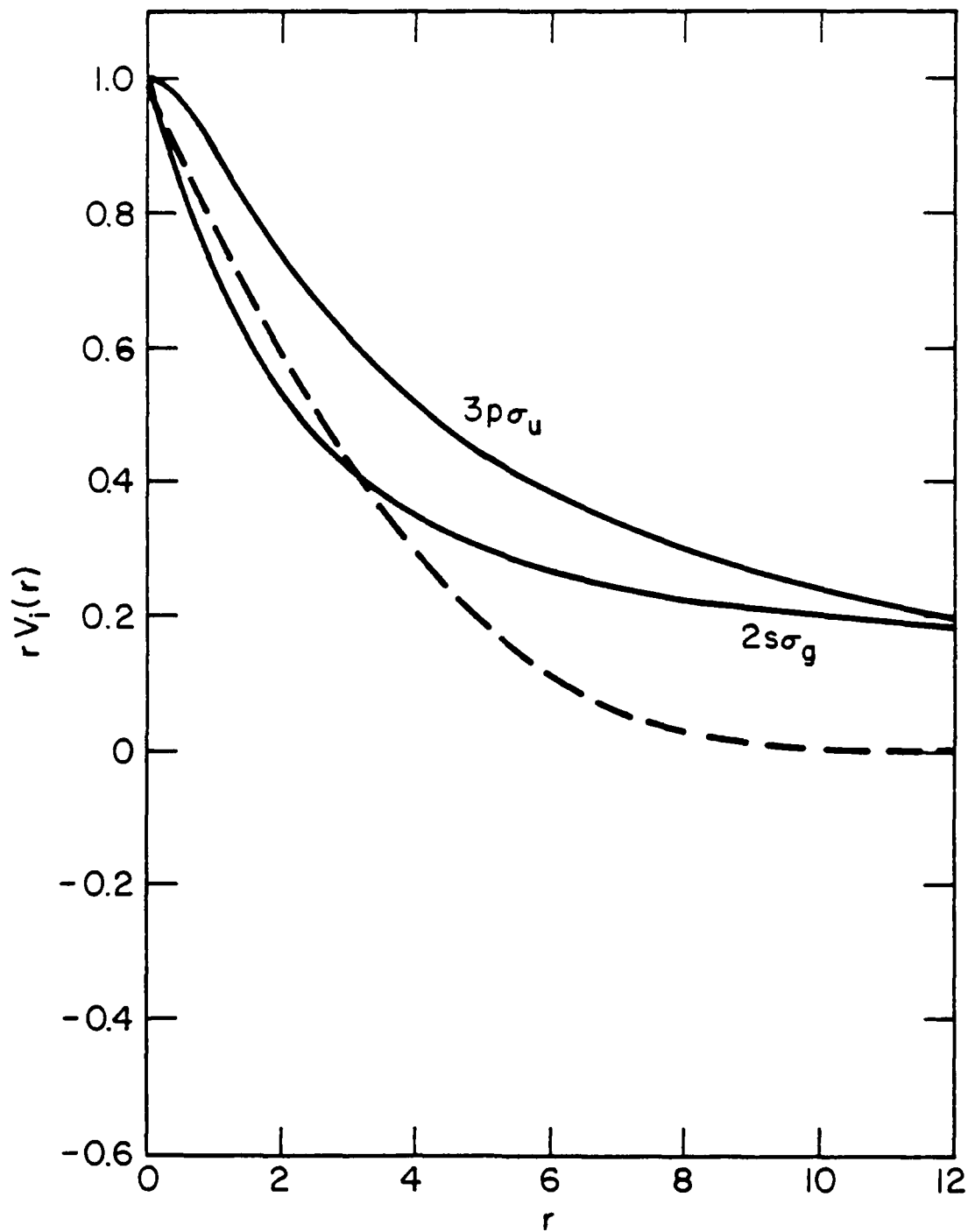
Fig. 6. Effective charge acting on the proton in the systems $H(2s) + H^{+}$. Full curves: V_i from Ref. 15. Dashed curve: V_i from screening by the 2s electron.
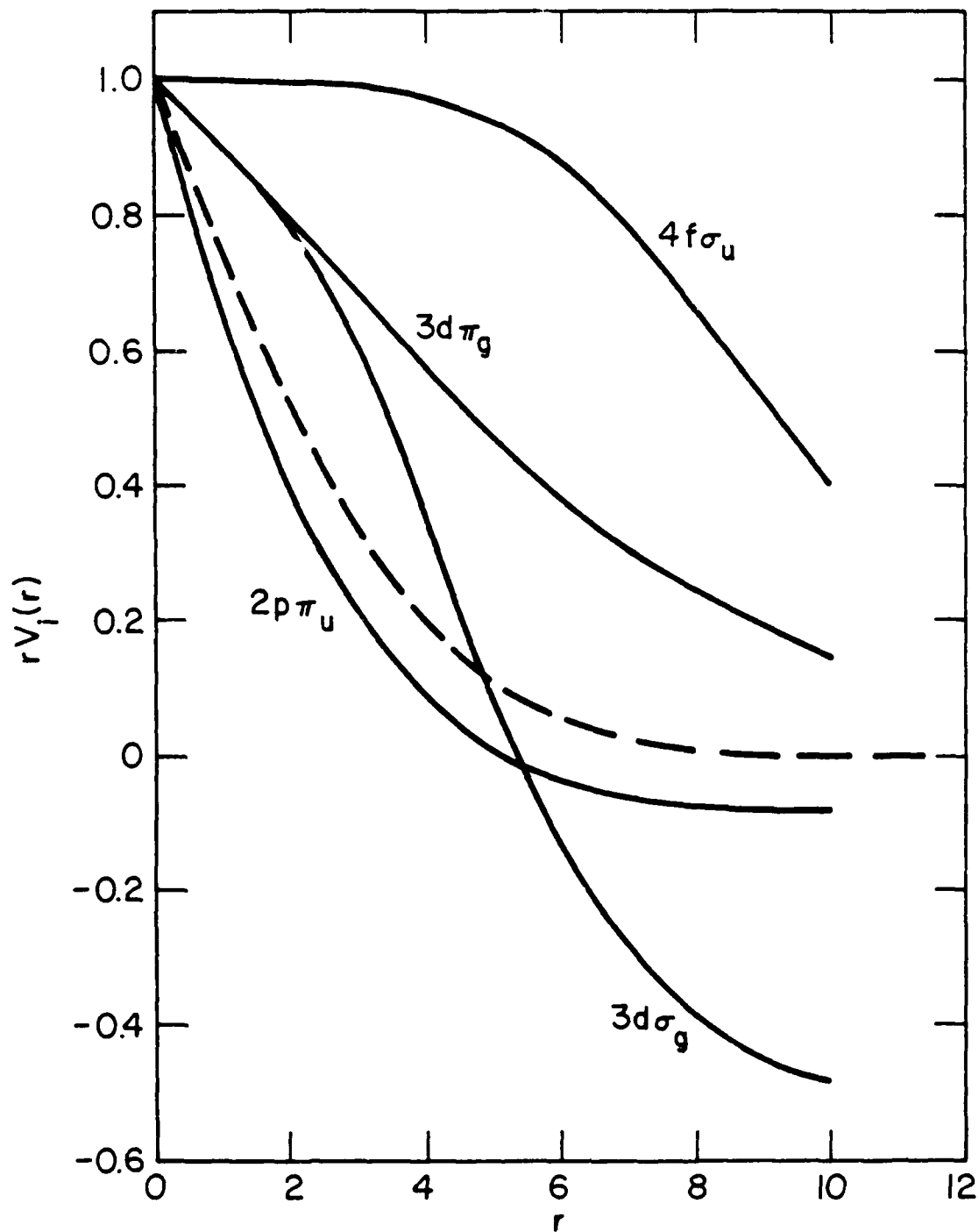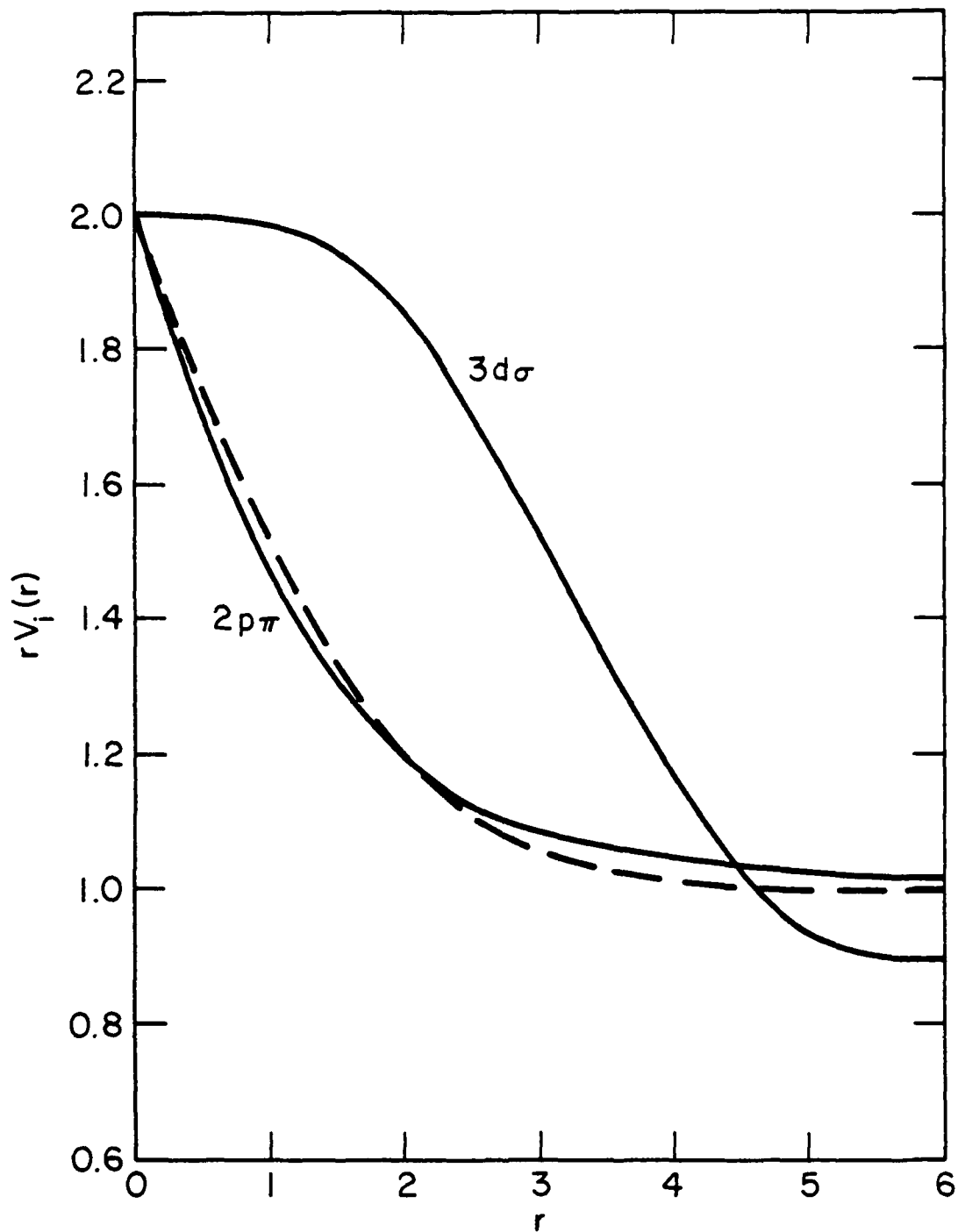
Fig. 7. Effective charge acting on the proton in the system H(2p) + H$^+$. Full curves: V_i from Ref. 15. Dashed curve: V_i from screening by the 2p electron.
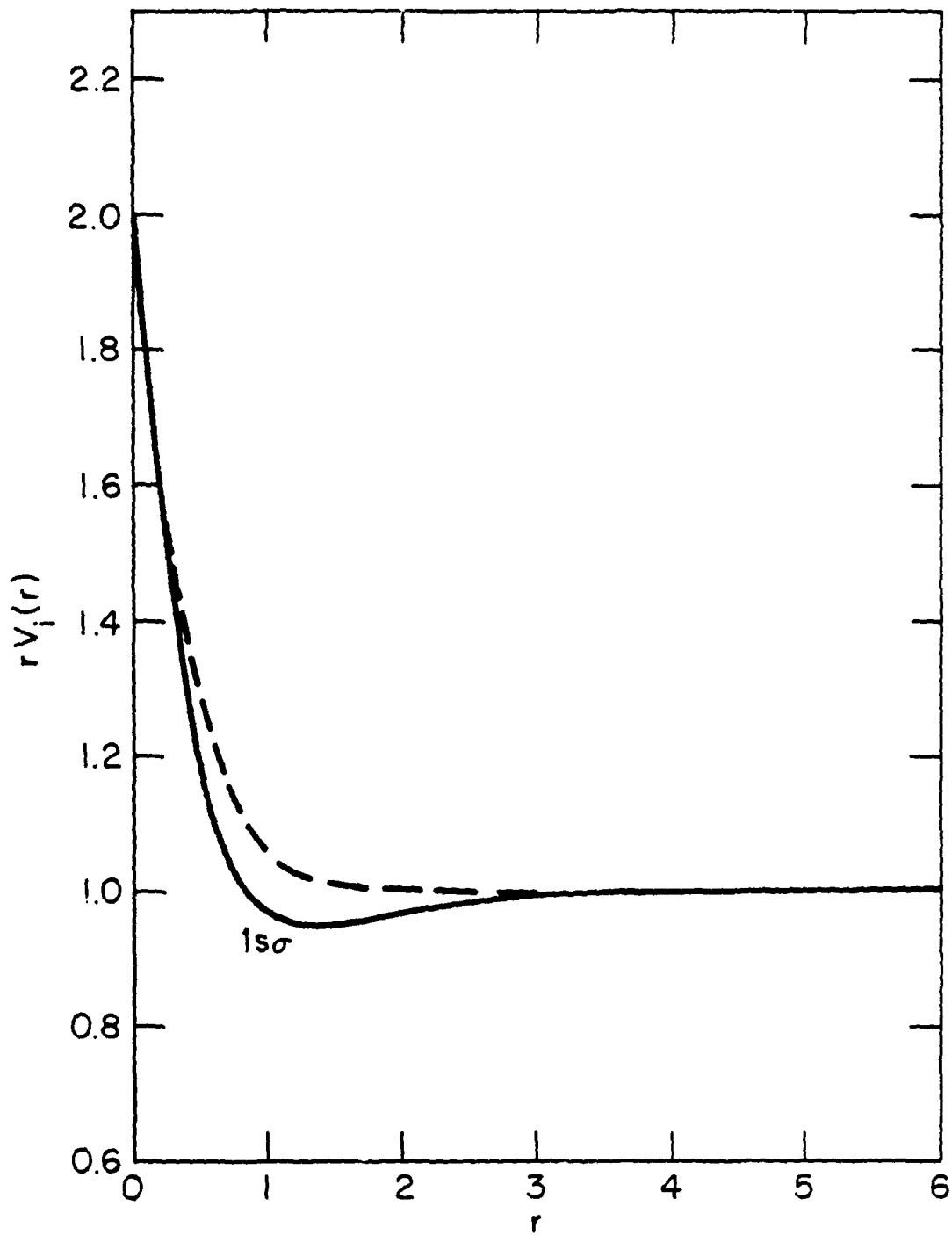
Fig. 8. Effective charge acting on the proton in the system $He^+(1s) + H^+$.
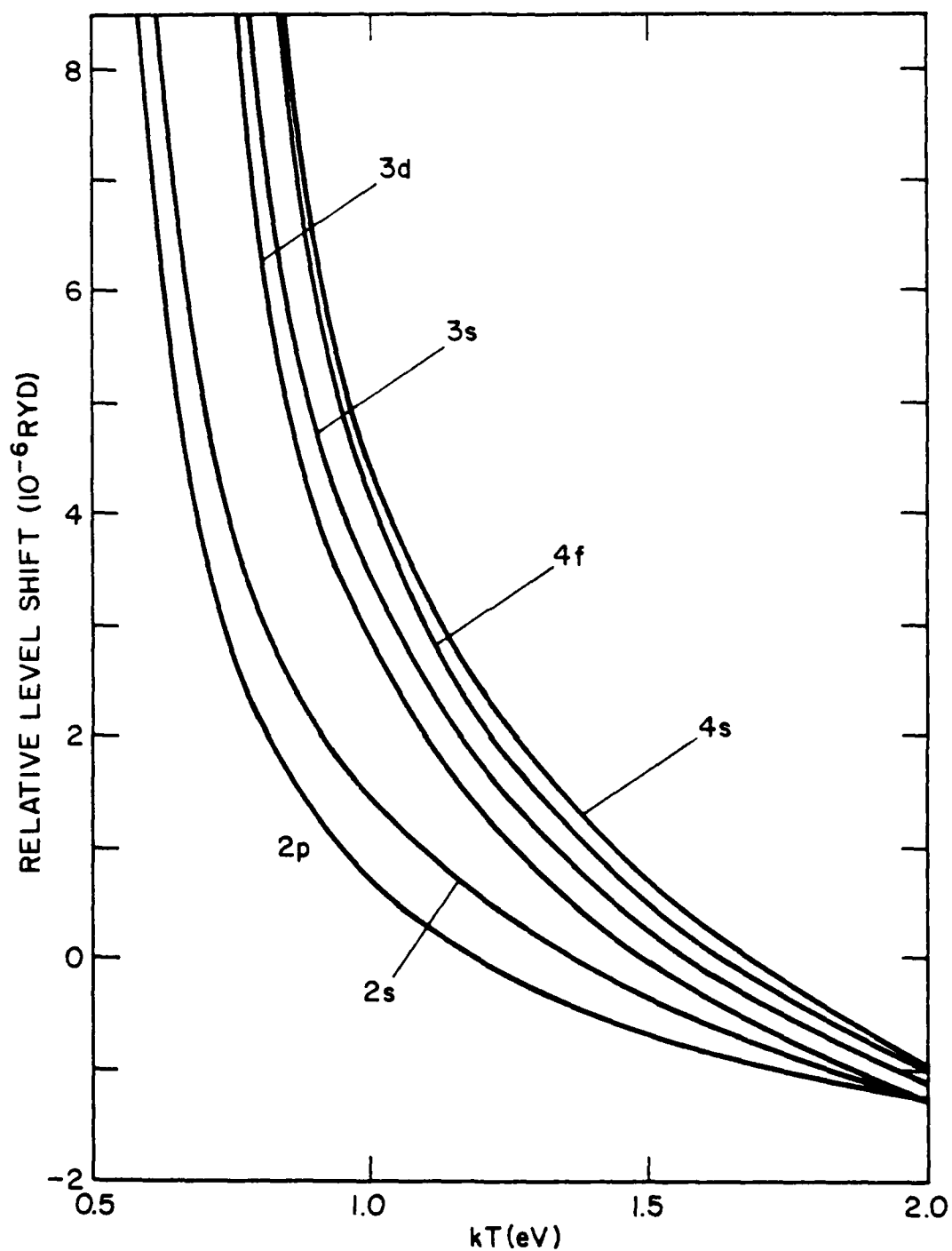Full curve: V_i from Ref. 14. Dashed curve: V_i from screening by the 1s
electron.
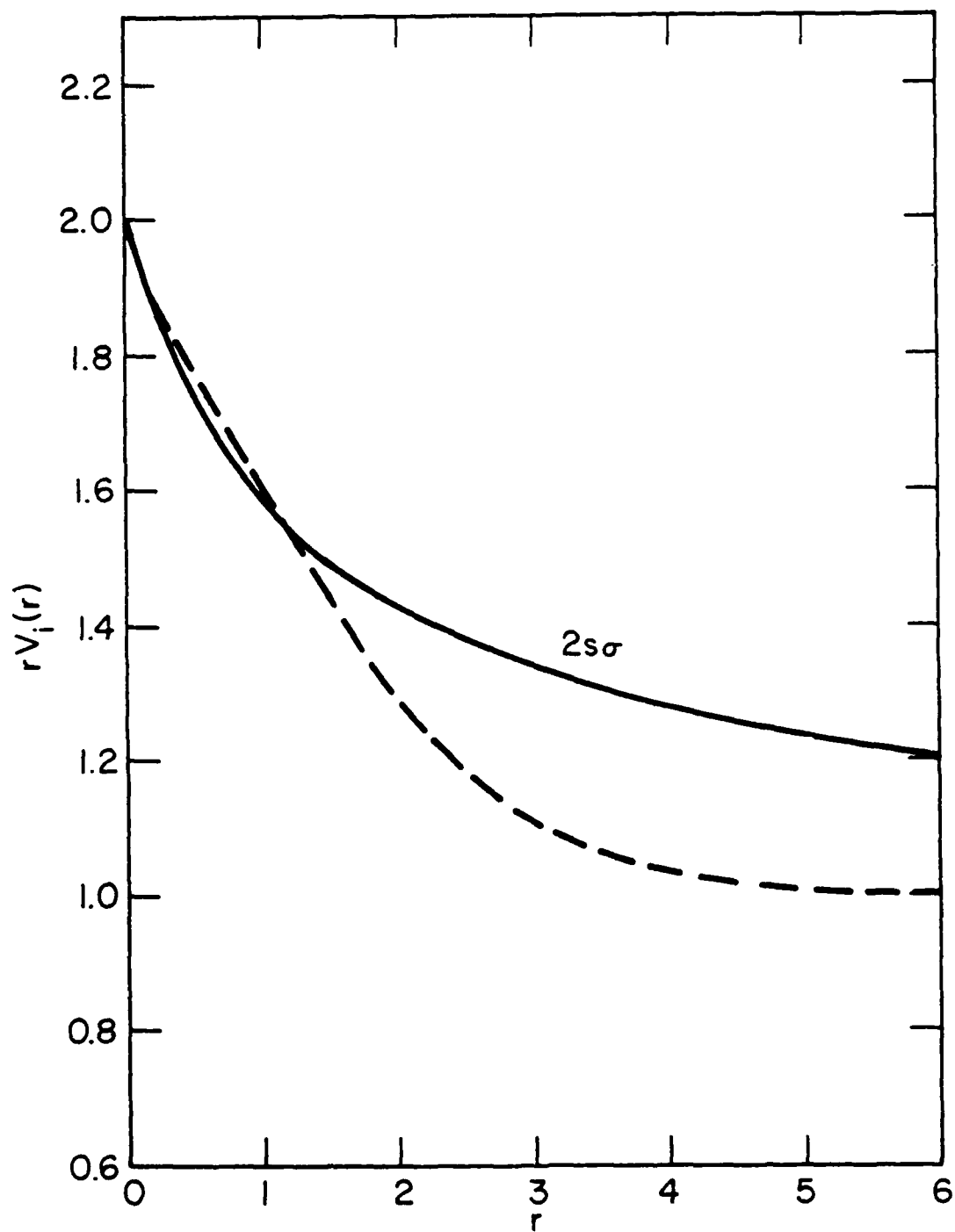
Fig. 9. Effective charge acting on the proton in the system $He^+(2s) + H^+$.
Full curve: V_i from Ref. 14. Dashed curve: V_i from screening by the 2s
electron.

Fig. 10. Effective charge acting on the proton in the system $He^+(2p) + H^+$. Full curves: V_i from Ref. 14. Dashed curve: V_i from screening by the 2p electron.

Fig. 11. Relative level shifts $\Delta E_{n\ell}^{-}$ for hydrogen. Hydrogen plasma, $N_e = 10^{17} cm^{-3}$. Case A (Same as in Fig. 1, but the proton distribution is derived from interatomic potentials corresponding to H(1s) + H$^+$ shown in Fig. 5). The curve for 3p lies between those for 3s and 3d, and the curves for 4p and 4d lie between 4s and 4f. They are not shown for clarity.
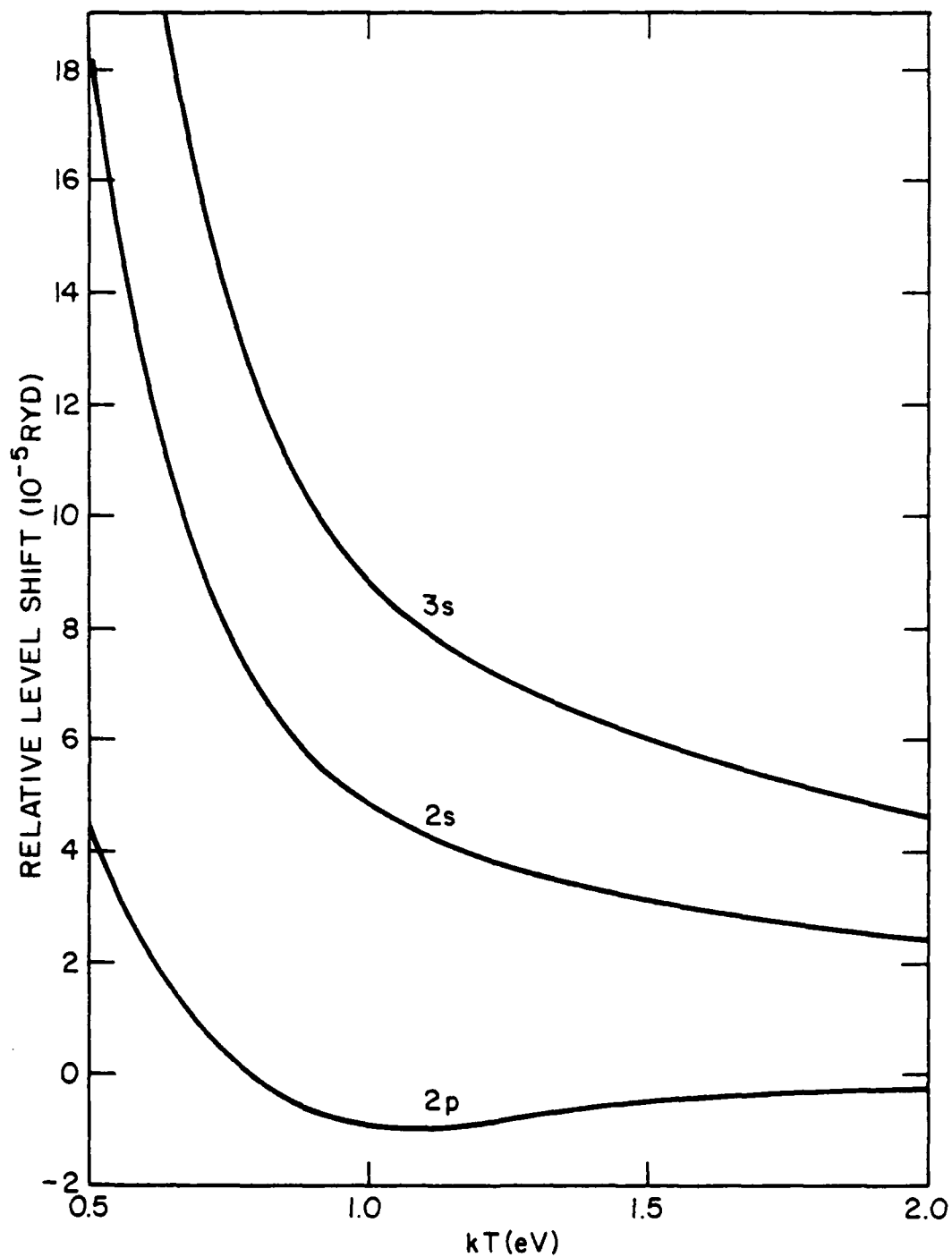
Fig. 12. Relative level shifts $\Delta E_{n\ell}^-$ for hydrogen. Hydrogen plasma, $N_e = 10^{17} cm^{-3}$. Case B (Same as in Fig. 2, but the proton distribution is derived from interatomic potentials corresponding to $H(2s) + H^+$, $H(2p) + H^+$, and $H(3s) + H^+$, respectively).
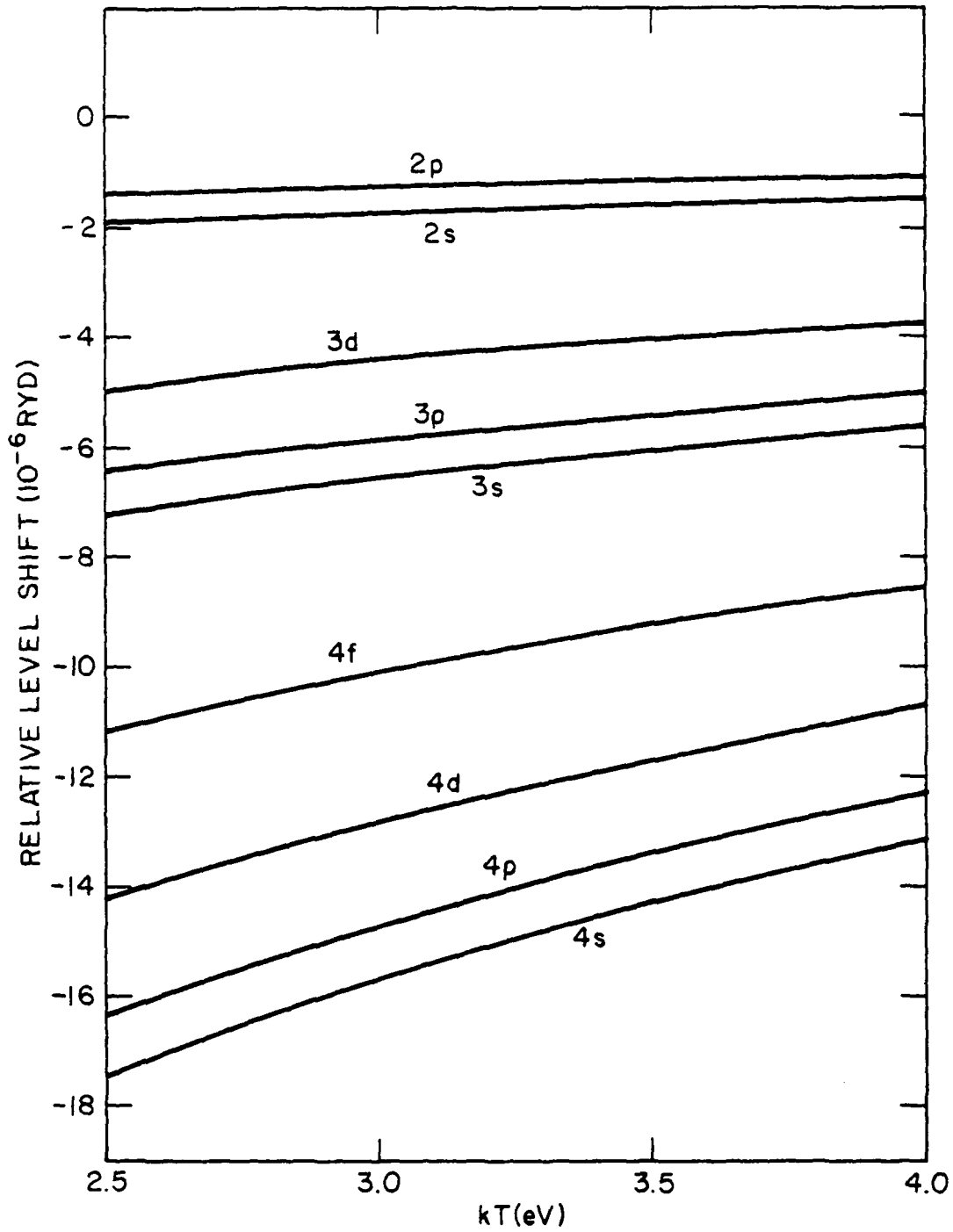
Fig. 13. Relative level shifts $\Delta E'_{n\ell}$ for ionized helium in a hydrogen plasma, $N_e = 10^{17} \text{cm}^{-3}$. Case A (Same as in Fig. 1, but the proton distribution is derived from the interatomic potential corresponding to $He^+(1s) + H^+$ shown in Fig. 8).

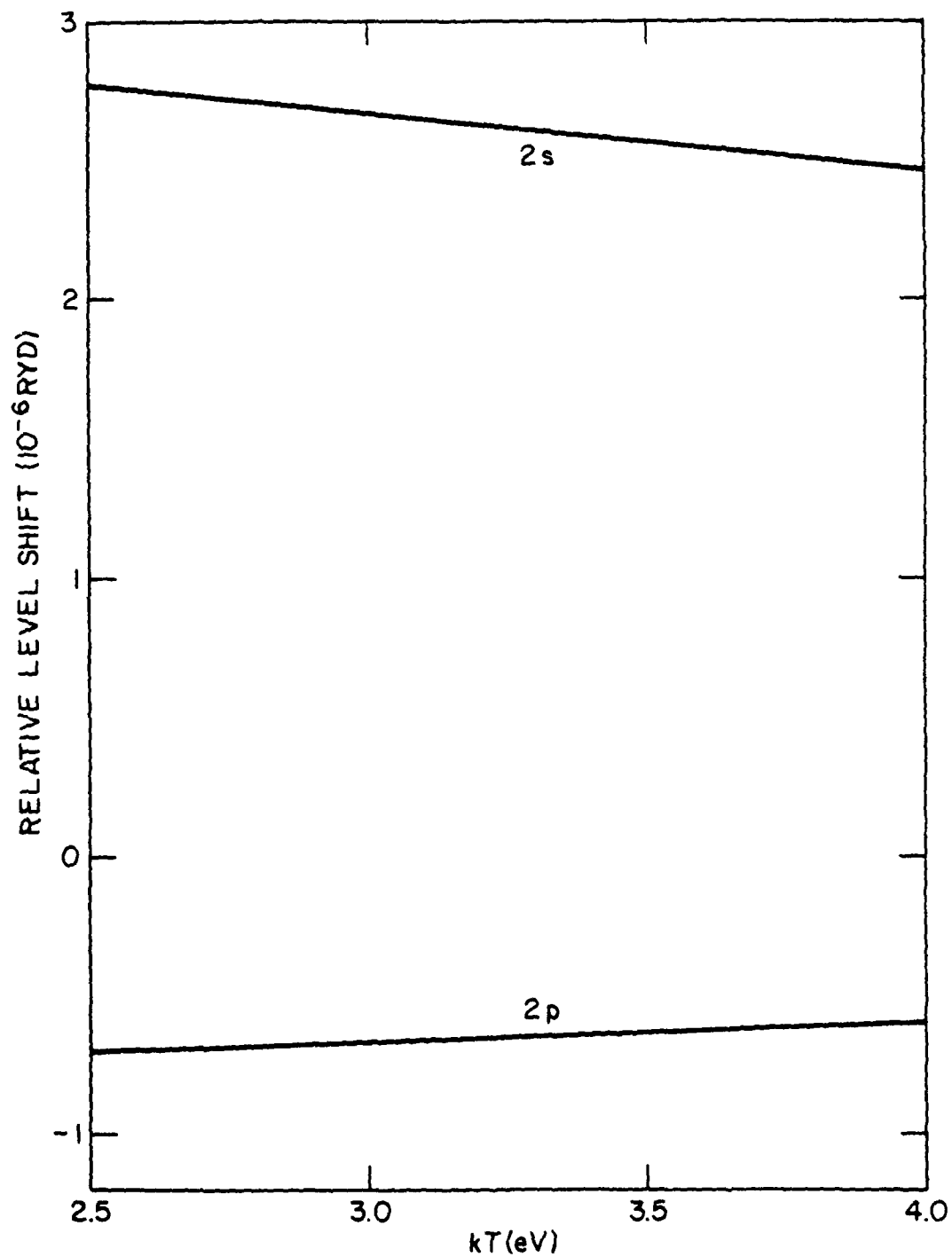Fig. 14. Relative level shifts $\Delta E_{n\ell}^-$ for ionized helium in a hydrogen plasma, $N_e = 10^{17} cm^{-3}$. Case B (same as in Fig. 2, but the proton distribution is derived from interatomic potentials corresponding to $He^+(2s) + H^+$ and $He^+(2p) + H^+$, respectively, shown in Figs. 9 and 10).

28